Atomistic basis for the plastic yield criterion of metallic glass

CHRISTOPHER A. SCHUH* AND ALAN C. LUND
Department of Materials Science and Engineering, Massachusetts Institute of Technology, 77 Massachusetts Avenue, Cambridge, Massachusetts 02139, USA
*e-mail: schuh@mit.edu

Published online: 8 June 2003; doi:10.1038/nmat918

Because of their disordered atomic structure, amorphous metals (termed metallic glasses) have fundamentally different deformation mechanisms compared with polycrystalline metals. These different mechanisms give metallic glasses high strength, but the extent to which they affect other macroscopic deformation properties is uncertain. For example, the nature of the plastic-yield criterion is a point of contention, with some studies reporting yield behaviour roughly in line with that of polycrystalline metals, and others indicating strong fundamental differences. In particular, it is unclear whether pressure- or normal stress-dependence needs to be included in the plastic-yield criterion of metallic glasses, and how such a dependence could arise from their disordered structure[1–4]. In this work we provide an atomic-level explanation for pressure-dependent yield in amorphous metals, based on an elementary unit of deformation. This simple model compares favourably with new atomistic simulations of metallic glasses, as well as existing experimental data.

In polycrystalline metals, the fundamental unit of plastic deformation is the motion of an individual dislocation. Because dislocations generally interact only weakly with a pressure field[5], the yield criterion for most metals is based on the maximum shear stress. Two well-known criteria that are used in this case are those of Tresca and von Mises, the latter of which accurately matches experimental data for a variety of metals and alloys[6]. An important characteristic of these yield criteria is their symmetry, predicting yield stresses of equal magnitude in either tension or compression. In contrast, metallic glasses have displayed asymmetric yield behaviour in several experimental studies[2,7], and it has been suggested that a different yield criterion is required for these materials. In particular, the Mohr–Coulomb criterion has been suggested as an alternative description that depends not only on the applied shear stress, τ, but also on the stress normal to the shear displacement, σ_n:

$$\tau_y = \tau_0 - \alpha\sigma_n \,. \tag{1}$$

Here, τ_y is the effective shear yield stress, τ_0 is a constant, and α is a system-specific coefficient that controls the strength of the normal stress effect. Physically, the form of equation (1) was originally proposed for granular materials, where the σ_n term arises from the geometric rearrangement of sliding particles and the friction between them, and thus α is an effective coefficient of friction. It has been postulated that equation (1) may apply to amorphous metals, because the relative motion of randomly packed atoms in a metallic glass is analogous to that of randomly packed particles in a granular solid[1,8]. However, the available experimental data are limited and, to our knowledge, there has been no theoretical underpinning of equation (1) for metallic glasses, which we seek to provide in this work.

According to the prevailing theory of plastic flow in metallic glasses[9–12], the fundamental unit of plasticity in amorphous metals is the shear transformation zone (STZ), which is a small cluster of randomly close-packed atoms that spontaneously and cooperatively reorganize under the action of an applied shear stress. A two-dimensional schematic is given in Fig. 1a, which shows how an STZ can accommodate a small increment of shear strain. The continued propagation of shear strain occurs by a process of self-assembly: the operation of one STZ creates a localized distortion of the surrounding material, and triggers the autocatalytic formation of large planar bands of STZs, commonly called shear bands.

Because the STZ has proved valuable for describing most of the important deformation physics of metallic glasses, we begin by considering a very simple STZ composed of nine close-packed atoms, as illustrated in Fig. 1b, and examine the effect that an applied normal stress σ_n has on the shear deformation of this unit. For this highly idealized system, the stress components are calculated using the usual approach[13]:

$$\sigma_n = \frac{1}{2V}\sum_{i=1}^{N}\sum_{\substack{j=1,\\ j\neq i}}^{N}\frac{\partial\varphi}{\partial r}\cdot\frac{(r_{ij}^{n})^2}{r_{ij}} \tag{2a}$$

$$\tau = \frac{1}{2V}\sum_{i=1}^{N}\sum_{\substack{j=1,\\ j\neq i}}^{N}\frac{\partial\varphi}{\partial r}\cdot\frac{r_{ij}^{n}\cdot r_{ij}^{t}}{r_{ij}} \tag{2b}$$

in which V is the system volume, φ is the interatomic potential, r_{ij} is the distance between atoms i and j, the superscripts n and t refer to normal and transverse components of the atomic separations, respectively, and N is the number of atoms in the system.

If no normal stress is applied (that is, $\sigma_n = 0$) and no thermal activation is allowed, then the shear displacement of the atoms as shown in Fig. 1b requires an applied shear stress that varies with position, as shown in Fig. 1c. On this curve, the maximum value of τ occurs before the atoms reach the saddle-point configuration, and is equal to the

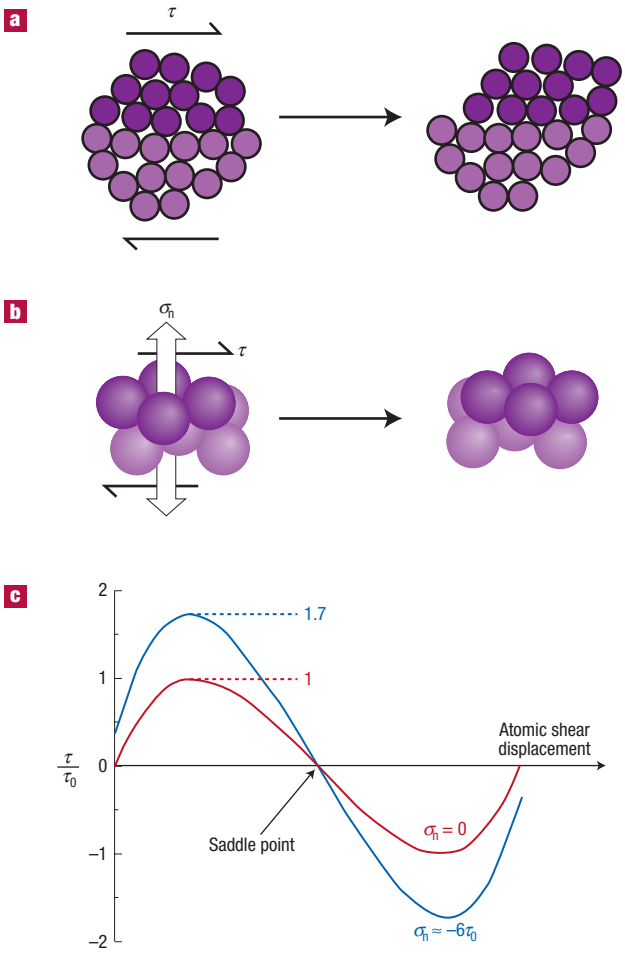

Figure 1 Shear transformation zones in metallic glasses. a, A two-dimensional schematic of a shear transformation zone in an amorphous metal. A shear displacement occurs to accommodate an applied shear stress τ, with the darker upper atoms moving with respect to the lower atoms (after ref. 9). **b**, A representation of the elementary three-dimensional shear transformation zone used in this study. The four upper (darker) atoms move as a unit with respect to the five lower atoms, and a trajectory with constant normal-stress σ_n is determined in the shear direction. **c**, The applied shear stress τ necessary to maintain a given atomic shear displacement, normalized by the maximum value of τ at $\sigma_n = 0$, τ_0. The beginning and end of the curve correspond to the starting and ending structures seen in **b**. The maximum value of τ necessary to complete the shear displacement of **b** increases with an applied compressive stress.

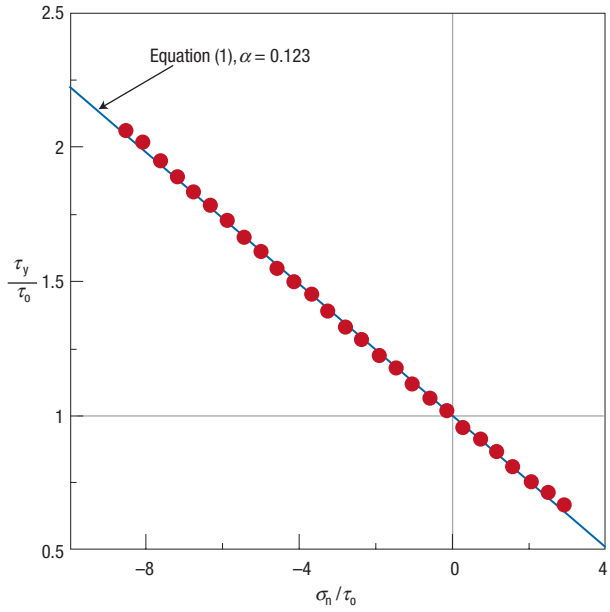

Figure 2 Fundamental yield criterion for an elementary shear transformation zone. The maximum normalized shear stress, τ_y/τ_0, required to translate the atoms of Fig. 1b from their beginning to their end state, for a constant applied normal stress, σ_n/τ_0. The data show an excellent fit to equation (1) with $\alpha = 0.123$, providing a physical basis for the Mohr–Coulomb yield criterion.

shear-yield stress. The curve in Fig. 1c has been calculated (see Methods) using Lennard–Jones potentials for the Cu–Zr atomic interaction[14], which is relevant for comparison with our larger simulations discussed later.

The approach described above can be extended to consider the effect of applied normal stress by solving equation (2) for a shear displacement across the saddle point where σ_n is constant at a prescribed value (see Methods). An example, with $\sigma_n \approx -6\tau_0$, is also shown in Fig. 1c. For this large applied compressive stress on the shear plane, the shear stress required to permanently deform the STZ increases by a factor of about 1.7. By repeating this calculation for multiple values of σ_n, we derive a direct relationship between τ_y and σ_n, as shown in Fig. 2. For a physically reasonable range of both tensile and compressive applied stresses, these data unequivocally fit a single line with the form of equation (1). Furthermore, this simple model provides a quantitative prediction for the friction coefficient α; for Cu–Cu, Zr–Zr, or Cu–Zr interaction potentials we find $\alpha = 0.123 \pm 0.004$. We have also used other physically realistic potentials, as well as various atomic arrangements and boundary conditions different from those in Fig. 1b (see Methods), and in all cases we observe the same fundamental response. Common metallic interaction potentials result in atomistic friction, and therefore the operation of STZs is governed by the Mohr–Coulomb criterion.

Because STZs are frequently observed in large-scale molecular simulations of amorphous systems[15–17], and because the above developments show that STZs obey the Mohr–Coulomb criterion, we speculate that this same behaviour will be observed at larger length scales. To test this hypothesis, we have conducted atomistic simulations of $Cu_{50}Zr_{50}$ metallic glasses composed of several thousand atoms. Using a fully periodic three-dimensional simulation cell with standard energy-minimization algorithms[18–20], we perform molecular statics computations using the same Lennard–Jones potentials as in the small system above. By controlling the relative strain increments in all three principle directions (denoted x, y and z)[21], we perform plane-stress simulations ($\sigma_{zz} = 0$) designed to probe the entire yield surface in the σ_{xx}–σ_{yy} plane (see Methods for more details).

A complete map of the biaxial yield surface derived from our simulations is shown in Fig. 3. The most striking feature of this data set is its pronounced asymmetry from tensile to compressive loading. For example, the asymmetry between pure tension and compression is approximately 25%, and the biaxial tensile and compressive lobes in quadrants I and III, respectively, exhibit a commensurate imbalance. As discussed above, this asymmetry is inconsistent with any yield criterion based only on maximum shear stress, including the Tresca and von Mises criteria common to polycrystalline materials. However, tension–compression asymmetry is characteristic of the Mohr–Coulomb criterion of equation (1). For comparison with the simulation data, the plane-stress Mohr–Coulomb yield surface is also included in Fig. 3; following our earlier analysis of an individual STZ,

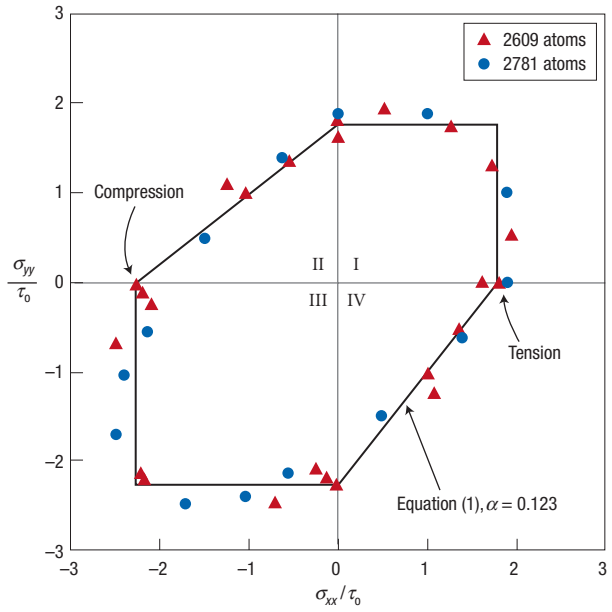

Figure 3 Yield surface of a metallic glass. Normalized principle stresses σ_{xx} and σ_{yy} at yield ($\sigma_{zz} = 0$) extracted from computational multiaxial mechanical tests. Data for two different amorphous structures are shown, composed of 2609 and 2781 atoms, respectively. The solid line is the Mohr–Coulomb yield criterion, equation (1), plotted with the value of $\alpha = 0.123$ obtained from the elementary shear transformation zone analysis of Fig. 2.

we use as input the value $\alpha = 0.123$ obtained for the Cu–Zr system. The conformity between the simulation data and the Mohr–Coulomb yield surface is very good.

We note that where the Mohr–Coulomb criterion considers the role of normal stresses on shear yield, there are other criteria based on the Tresca or von Mises criteria that make a similar attempt to account for tension–compression asymmetry by including a hydrostatic pressure term (for example, ref. 22). These criteria can be stated in a similar form to equation (1), but use the hydrostatic pressure in place of the normal stress σ_n. These various criteria are all inherently similar to the Mohr–Coulomb criterion, and as such, could likely fit the data in Fig. 3 with reasonable accuracy. However, based on our analysis in Fig. 2, we believe that the physical origin of this effect in metallic glasses lies in the principle of 'atomistic friction', as embodied in the Mohr–Coulomb criterion, and therefore only compare the simulation results to that criterion here.

The excellent mutual agreement between equation (1), the STZ analysis in Fig. 2, and the simulation data in Fig. 3, provides a strong physical basis for the Mohr–Coulomb yield criterion in metallic glasses. These theoretical results are also in good agreement with the available experimental data from a variety of metallic glasses. For example, mechanical tests on a $Pd_{40}Ni_{40}P_{20}$ metallic glass were conducted[23] using various multiaxial stress states, and it was found that the data were best described by the Mohr–Coulomb criterion with $\alpha = 0.11 \pm 0.03$. More recently, instrumented indentation experiments on a Zr-based glass were performed[8], and finite-element simulations showed that the data could best be described using the Mohr–Coulomb criterion with $\alpha = 0.13$. The value of $\alpha = 0.123 \pm 0.004$ found in our analyses above matches these experimental values quite well.

Further contact can be made with experimental data on the basis of shear-band angles measured in simple uniaxial tests. For Tresca or von Mises yielding of a compression specimen, this angle would be expected to lie at $\theta = 45°$ to the compression axis, whereas the Mohr–Coulomb criterion predicts a smaller angle given implicitly by[8]:

$$\alpha = \frac{\cos(2\theta)}{\sin(2\theta)} \quad . \tag{3}$$

Using the value of $\alpha = 0.123 \pm 0.004$ found in our analyses above, equation (3) predicts a compressive shear angle of $\theta = 41.5 \pm 0.15°$. This value is in agreement with previous experimental results[2] with a range of $\theta = 39.5$–$43.7°$ for a variety of metallic glass compositions.

To summarize the above discussion, we find that simulated amorphous metals plastically yield in a manner consistent with the Mohr–Coulomb criterion. Using a fundamental model of shear atomic shuffles, we show that this behaviour is intrinsic to the atomic-scale processes involved in metallic glass deformation. This simple approach agrees remarkably well with our larger-scale atomistic simulations and a variety of independent experiments. Given the current ambiguity on this issue in the experimental literature, we believe that our analysis provides convincing support for the Mohr–Coulomb criterion, and propose that future studies on metallic glass should be carried out within the framework of such a pressure- or normal stress-dependent yield criterion. The resulting asymmetric yield behaviour has broad implications for structural applications of metallic glasses, because these materials can be expected to be uniformly weaker in tension than they are in compression, regardless of future advances in compositional control. It will also be necessary to consider this asymmetry in the design of amorphous-matrix metallic composites, which are widely sought after for improved ductility[24,25].

As a final note, we suggest that these considerations may also have significant implications for nanostructured materials, in addition to metallic glasses. The lowest physical limit for nanostructure length scales is the amorphous state[26], and molecular simulations show that the deformation mechanisms of polycrystalline materials diverge from typical behaviour in the nanostructural range[21,27]. Although we know of no experimental or computational investigations that consider the yield surface of nanocrystalline materials, we predict a transition from dislocation-dominated yield processes (following the von Mises criterion) to STZ-dominated yield (following the Mohr–Coulomb criterion) as grain size decreases toward zero.

METHODS

NINE-ATOM STZ MODEL

We determine the stress components given by equation (2) for simple shear shuffles of the nine-atom model shown in Fig. 1b. Here the atoms are initially in a close-packed configuration, with four atoms in the upper plane, and five atoms below. The upper plane is then moved as a rigid unit relative to the lower plane, with the position of this unit being specified by a single vector away from the initial position. We calculate the stresses σ_n and τ for every vector in a three-dimensional space within 1.5 interatomic distances of the initial configuration. We then identify trajectories of constant σ_n that connect the initial and final close-packed configurations, and cross the saddle-point configuration. The shear stress τ calculated at every point along this constant-σ_n-trajectory describes a curve such as those shown in Fig. 1c. We have performed these calculations for several boundary conditions, including the free-boundary conditions shown in Fig. 1b,c, where the nine atoms are isolated in space, as well as the shearing of infinite close-packed sheets. We find that due to the symmetry and periodicity of the nine-atom unit, any reasonable boundary conditions yield similar results and are not critical to the fundamental form of the curves. Finally, we have also considered other STZ geometries, including the four-atom model of Falk[16] (who did not consider the normal stress dependence of the shear transformation), and in all cases we find that equation (1) is strictly obeyed at the atomic level.

MOLECULAR STATICS SIMULATIONS

For larger-scale molecular simulations, we use the method of conjugate gradients to relax atoms to their local equilibrium positions, within a simulation cell periodic in all three dimensions. The potentials are those cited in the text, and also used in the smaller nine-atom STZ model described above. For multiaxial testing, we apply small increments of strain in the principle directions, relocating each atom by a self-affine transformation of coordinates; strain increments may not exceed 0.1%. Stresses are calculated with equations similar to those of equation (2), generalized to determine each component of the stress tensor[13]. The resulting stress–strain curves are linear elastic at low strains and fully plastic at high strains, with a gradual transition between. The yield point lies in this transition region, and numerical values for the yield-stress components are extracted from the data using a standard linear offset method[22]. Full data sets from these simulations will be reported elsewhere.

The molecular simulation results presented in Fig. 3 have also been extensively corroborated by additional computations whose analysis we omit here for brevity. For example, we have studied systems with sizes from a few hundred to several thousand atoms, and find no fundamental deviation from the results presented here. Additionally, we have used not only fully periodic boundary conditions, but have also considered a three-dimensional cell that is periodic in only two dimensions (equivalent to biaxial testing of an infinite thin sheet). Again, the boundary condition had no fundamental effect on our conclusions about the yield criterion. Finally, we have used several different sets of interatomic potentials in addition to those presented in Fig. 3, and found the same results. Further details of these variations and our methods will be reported elsewhere.

Received 7 February 2003; accepted 6 May 2003; published 8 June 2003.

References

1. Lewandowski, J. J. & Lowhaphandu, P. Effects of hydrostatic pressure on the flow and fracture of a bulk amorphous metal. *Phil. Mag. A* **82,** 3427–3441 (2002).
2. Zhang, Z. F., Eckert, J. & Schultz, L. Difference in compressive and tensile fracture mechanisms of $Zr_{59}Cu_{20}Al_{10}Ni_8Ti_3$ bulk metallic glasses. *Acta Mater.* **51,** 1167–1179 (2003).
3. Flores, K. M. & Dauskardt, R. H. Mean stress effects on flow localization and failure in a bulk metallic glass. *Acta Mater.* **49,** 2527–2537 (2001).
4. Lowhaphandu, P., Montgomery, S. L. & Lewandowski, J. J. Effects of superimposed hydrostatic pressure on flow and fracture of a Zr-Ti-Ni-Cu-Be bulk amorphous alloy. *Scripta Mater.* **41,** 19–24 (1999).
5. Bulatov, V. V., Richmond, O. & Glazov, M. V. An atomistic dislocation mechanism of pressure-dependent plastic flow in aluminum. *Acta Mater.* **47,** 3507–3514 (1999).
6. Courtney, T. H. *Mechanical Behaviour of Materials* (McGraw-Hill, New York, 1990).
7. Mukai, T., Nieh, T. G., Kawamura, Y., Inoue, A. & Higashi, K. Effect of strain rate on compressive behaviour of a $Pd_{40}Ni_{40}P_{20}$ bulk metallic glass. *Intermetall.* **10,** 1071–1077 (2002).
8. Vaidyanathan, R., Dao, M., Ravichandran, G. & Suresh, S. Study of mechanical deformation in bulk metallic glass through instrumented indentation. *Acta Mater.* **49,** 3781–3789 (2001).
9. Argon, A. S. Plastic deformation in metallic glasses. *Acta Metall.* **27,** 47–58 (1979).
10. Spaepen, F. A microscopic mechanism for steady state inhomogeneous flow in metallic glasses. *Acta Metall.* **25,** 407–415 (1977).
11. Eastgate, L. O., Langer, J. S. & Pechenik, L. Dynamics of large-scale plastic deformation and the necking instability in amorphous solids. *Phys. Rev. Lett.* **90,** 045506 (2003).
12. Kim, J.-J., Choi, Y., Suresh, S. & Argon, A. S. Nanocrystallization during nanoindentation of a bulk amorphous metal alloy at room temperature. *Science* **295,** 654–657 (2002).
13. Born, M. & Huang, K. *Dynamical Theory of Crystal Lattices* (Claredon, Oxford, UK, 1954).
14. Kobayashi, S., Maeda, K. & Takeuchi, S. Computer simulation of deformation of amorphous $Cu_{57}Zr_{43}$. *Acta Metall.* **28,** 1641–1652 (1980).
15. Falk, M. L. & Langer, J. S. Dynamics of viscoplastic deformation in amorphous solids. *Phys. Rev. E* **57,** 7192–7205 (1998).
16. Falk, M. L. Molecular-dynamics study of ductile and brittle fracture in model noncrystalline solids. *Phys. Rev. B* **60,** 7062–7070 (1999).
17. Argon, A. S. & Kuo, H. Y. Plastic flow in a disordered bubble raft (an analog of a metallic glass). *Mater. Sci. Eng.* **39,** 101–109 (1979).
18. Lund, A. C. & Schuh, C. A. Atomistic simulation of strain-induced amorphization. *Appl. Phys. Lett.* **82,** 2017–2019 (2003).
19. Lacks, D. J. Energy landscape and the non-newtonian viscosity of liquids and glasses. *Phys. Rev. Lett.* **87,** 225502 (2001).
20. Gagnon, G., Patton, J. & Lacks, D. J. Energy landscape view of fracture and avalanches in disordered materials. *Phys. Rev. E* **64,** 051508 (2001).
21. Schiotz, J., Vegge, T., Tolla, F. D. D. & Jacobsen, K. W. Atomic-scale simulations of the mechanical deformation of nanocrystalline metals. *Phys. Rev. B* **60,** 11971–11983 (1999).
22. Rottler, J. & Robbins, M. O. Yield conditions for deformation of amorphous polymer glasses. *Phys. Rev. E* **64,** 051801 (2001).
23. Donovan, P. E. A yield criterion for $Pd_{40}Ni_{40}P_{20}$ metallic glass. *Acta Mater.* **37,** 445–456 (1989).
24. Fan, C., Ott, R. T. & Hufnagel, T. C. Metallic glass matrix composite with precipitated ductile reinforcement. *Appl. Phys. Lett.* **81,** 1020–1022 (2002).
25. Hays, C. C., Kim, C. P. & Johnson, W. L. Microstructure controlled shear band pattern formation and enhanced plasticity of bulk metallic glass containing in situ formed ductile phase dendrite dispersions. *Phys. Rev. Lett.* **84,** 2901–2904 (2000).
26. Nieh, T. G. & Wadsworth, J. Hall-Petch relation in nanocrystalline solids. *Scripta Metall. Mater.* **25,** 955–958 (1991).
27. Yamakov, V., Wolf, D., Phillpot, S. R., Mukherjee, A. K. & Gleiter, H. Dislocation processes in the deformation of nanocrystalline aluminium by molecular-dynamics simulation. *Nature Mater.* **1,** 1–4 (2002).

Acknowledgements

This work was partially supported by the Defense University Research Initiative on NanoTechnology (DURINT) on damage and failure resistant nanostructured materials, which is funded at the Massachusetts Institute of Technology by the US Office of Naval Research, Grant No. N00014-01-1-0808. Correspondence and requests for materials should be addressed to C.A.S.

Competing financial interests

The authors declare that they have no competing financial interests.